

Finite epidemic thresholds in fractal scale-free ‘large-world’ networks

Zhongzhi Zhang^{1,2 a}, Shuigeng Zhou^{1,2 b}, Tao Zou^{1,2}, and Jihong Guan³

¹ Department of Computer Science and Engineering, Fudan University, Shanghai 200433, China

² Shanghai Key Lab of Intelligent Information Processing, Fudan University, Shanghai 200433, China

³ Department of Computer Science and Technology, Tongji University, 4800 Cao’an Road, Shanghai 201804, China

Received: date / Revised version: date

Abstract. It is generally accepted that scale-free networks is prone to epidemic spreading allowing the onset of large epidemics whatever the spreading rate of the infection. In the paper, we show that disease propagation may be suppressed in particular fractal scale-free networks. We first study analytically the topological characteristics of a network model and show that it is simultaneously scale-free, highly clustered, “large-world”, fractal and disassortative. Any previous model does not have all the properties as the one under consideration. Then, by using the renormalization group technique we analyze the dynamic susceptible-infected-removed (SIR) model for spreading of infections. Interestingly, we find the existence of an epidemic threshold, as compared to the usual epidemic behavior without a finite threshold in uncorrelated scale-free networks. This phenomenon indicates that degree distribution of scale-free networks does not suffice to characterize the epidemic dynamics on top of them. Our results may shed light in the understanding of the epidemics and other spreading phenomena on real-life networks with similar structural features as the considered model.

PACS. 89.75.Hc Networks and genealogical trees – 87.19.Xx Diseases – 05.45.Df Fractals – 36.40.Qv Stability and fragmentation of clusters

1 Introduction

In the past ten years, there has been a considerable interest in characterizing and understanding the topological properties of networked systems [1, 2, 3, 4, 5]. It has been established that scale-free behavior [6] is one of the most fundamental concepts constituting our basic understanding of the organization of many real-world systems in nature and society. This scale-free property has a profound effect on almost every aspect on dynamic processes taking place on networks, including robustness [7], percolation [8, 9], synchronization [11], games [12], epidemic spreading [13, 14, 15], and so on. For instance, for a wide range of scale-free networks, there is no existence of an epidemic threshold, even infections with low spreading rate will prevail over the entire population in these networks [13, 14, 15]. This radically changes the conclusion drawn from classic disease modeling [16].

Recently, it has been discovered that many real-life networks, such as the WWW, metabolic networks, and yeast protein interaction networks have self-similar properties and exhibit fractal scaling [17, 18, 19, 20]. The fractal topology can be characterized through two exponents: fractal dimension d_B and degree exponent of the boxes

d_k , which can be obtained by box-counting algorithm [17, 18, 21, 22]. The scaling of the minimum number of boxes N_B of linear size ℓ_B needed to cover the network with node number N defines the fractal dimension d_B , namely $N_B/N \sim \ell_B^{-d_B}$. Analogously, the degree exponent of the boxes d_k is identified through $k_B(\ell_B)/k_{hub} \sim \ell_B^{-d_k}$, where $k_B(\ell_B)$ is the number of outgoing links from the box as a whole, and k_{hub} the largest node degree inside the box. Fractal networks are all self-similar, which means that fractal scale-free networks present the property of scale-invariance of degree distribution, $P(k) \sim k^{-\gamma}$, i.e., the exponent γ remains the same for different box sizes [17]. In self-similar scale-free networks, the three indexes γ , d_B and d_k satisfy the following relation: $\gamma = 1 + d_B/d_k$ [17].

As a fundamental property, topological fractality relates to many respects of network structure and function. Recent authors have shown that the correlation between degree and betweenness centrality of nodes is much weaker in fractal network models in comparison with non-fractal models [23]. It has been also shown [18, 19, 24] that fractal scale-free networks are not assortative, this disassortativity feature together with fractality makes such scale-free networks more robust against intentional attacks on hub nodes, as compared to the very vulnerable non-fractal scale-free networks [18]. In addition to the distinction in the robustness, fractal networks exhibit poorer synchrono-

^a e-mail: zhangzz@fudan.edu.cn

^b e-mail: sgzhou@fudan.edu.cn

nizability than non-fractal counterparts [24]. Although a lot of jobs have been devoted to characterizing fractal networks [25, 26, 27, 28, 29, 30], it is still of current interest to model fractal topology and seek a better understanding of its consequences on dynamic processes.

In this paper, we relate fractality to dynamics of disease spread in deterministic networks. Deterministic graphs have strong advantages. For example, they allow to compute analytically their properties, which have played a significant role, both in terms of explicit results and a guide to and a test of simulated and approximate methods [31, 32, 33, 34, 35, 36, 37, 38, 39, 40, 41, 42, 43, 44, 45, 46, 47, 48, 49, 50]. We first introduce a deterministic family of fractal graphs. From the viewpoint of complex networks, we determine accurately the topological characteristics of a particular graph and show that it is simultaneously scale-free, highly clustered, fractal and disassortative, but lacks the small-world property. Then we define a dynamic susceptible-infected-removed (SIR) model [16] on the two dimensional fractal graph to study the effect of fractality on disease spreading. By mapping the SIR model to a bond percolation problem, we found that there is an existence of finite epidemic threshold. Thus, the transmission rate needs to exceed a critical value for the disease to spread and prevail, which shows that the fractal networks are robust to infection.

2 Network construction and topologies

This section is devoted to the construction and the relevant structural properties of the studied network, such as degree distribution, clustering coefficient, average path length (APL), fractality, and correlations.

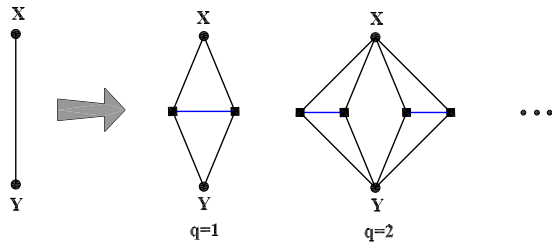


Fig. 1. (Color online) Iterative construction method of the fractal networks. Each iterative link is replaced by a connected cluster on the right-hand side of the arrow. The blue links are noniterated ones.

2.1 Construction algorithm

The proposed class of fractal networks is constructed in an iterative way as shown in Fig. 1. Let $F_{t,q}$ ($t \geq 0$, $q \geq 1$) denote the networks after t iterations. Then the networks

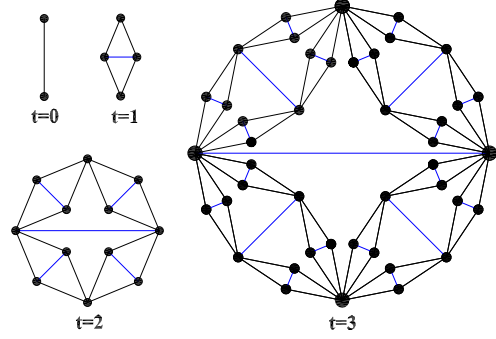


Fig. 2. (Color online) Scheme of the growth of the network for the particular case of $q = 1$. Only the first three iterative processes are shown.

are generated as follows: For $t = 0$, $F_{0,q}$ is an iterative edge connecting two nodes. For $t \geq 1$, $F_{t,q}$ is obtained from $F_{t-1,q}$. We replace each existing iterative edge in $F_{t-1,q}$ by a connected cluster of edges on the right of Fig. 1, where q denotes the number of the newly-created noniterated links induced by the iterative edge. The growing process is repeated t times, with the family of fractal graphs obtained in the limit $t \rightarrow \infty$. Figure 2 shows the growing process of the network for the particular case of $q = 1$. Note that all generated networks have qualitatively similar properties. In what follows we focus on the special case of $q = 1$ and denote it as F_t after t iterations.

Next we compute the numbers of total nodes (vertices) and links (edges) in F_t . Notice that there are two types of links (i.e., iterative links and noniterated links) in the network. Let $L_v(t)$, $L_i(t)$ and $L_n(t)$ be the number of new vertices, iterative links, and noniterated links created at step t , respectively. Since all old iterative links are not preserved in the growing process, thus $L_i(t)$ is in fact the total number of iterative links at time t . Note that each of the existing iterative links yields two nodes connected by one noniterated link, and the addition of each new node leads to two iterative links. By construction, for $t \geq 1$, we have

$$\begin{cases} L_i(t) = 4 L_i(t-1), \\ L_v(t) = 2 L_i(t-1), \\ L_n(t) = L_i(t-1). \end{cases} \quad (1)$$

Considering the initial condition $L_v(0) = 2$, $L_i(0) = 1$, and $L_n(0) = 0$, it follows that

$$\begin{cases} L_v(t) = 2 \cdot 4^{t-1}, \\ L_i(t) = 4^t, \\ L_n(t) = 4^{t-1}. \end{cases} \quad (2)$$

Thus the number of total nodes N_t and edges E_t present at step t is

$$N_t = \sum_{t_i=0}^t L_v(t_i) = \frac{2 \cdot 4^t + 4}{3} \quad (3)$$

and

$$E_t = L_i(t) + \sum_{t_i=1}^t L_n(t_i) = \frac{4^{t+1} - 1}{3}, \quad (4)$$

respectively. The average degree after t iterations is

$$\langle k \rangle_t = \frac{2 E_t}{N_t} = \frac{2(4^{t+1} - 1)}{2 \cdot 4^t + 4}, \quad (5)$$

which approaches 4 in the infinite t limit.

2.2 Degree distribution

When a new node u is added to the network at step t_u ($t_u \geq 1$), it has three links, among which two are iterative links and one is noniterated link. Let $L_i(u, t)$ be the number of iterative links at step t that will create new nodes connected to the node u at step $t + 1$. Then at step t_u , $L_i(u, t_u) = 2$. From the iterative generation process of the network, one can see that at any subsequent step each iterative link of u is broken and generates two new iterative links connected to u . We define $k_u(t)$ as the degree of node u at time t , then the relation between $k_u(t)$ and $L_i(u, t)$ satisfies:

$$k_u(t) = L_i(u, t) + 1, \quad (6)$$

where the last term 1 represents the only noniterated link of node u . Now we compute $L_i(u, t)$. By construction, $L_i(u, t) = 2 L_i(u, t - 1)$. Considering the initial condition $L_i(u, t_u) = 2$, we can derive $L_i(u, t) = 2^{t-t_u+1}$. Then at time t , the degree of vertex u becomes

$$k_u(t) = 2^{t-t_u+1} + 1. \quad (7)$$

It should be mentioned that the initial two nodes created at step 0 have a little different evolution process from other ones. Since the initial two nodes have no noniterated link, we can easily obtain that at step t , for either of the initial two nodes, its degree just equals the number of iterative links connecting it, both of which are 2^t .

Equation (7) shows that the degree spectrum of the network is discrete. It follows that the cumulative degree distribution [3] is given by

$$P_{\text{cum}}(k) = \sum_{\tau \leq t_u} \frac{L_v(\tau)}{N_t} = \frac{2 \cdot 4^{t_u} + 4}{2 \cdot 4^t + 4}. \quad (8)$$

Substituting for t_u in this expression using $t_u = t + 1 - \frac{\ln(k-1)}{\ln 2}$ gives

$$P_{\text{cum}}(k) = \frac{2 \cdot 4^t \cdot 4(k-1)^{-(\ln 4 / \ln 2)} + 4}{2 \cdot 4^t + 4}. \quad (9)$$

When t is large enough, one can obtain

$$P_{\text{cum}}(k) = 4(k-1)^{-2}. \quad (10)$$

So the degree distribution follows a power law form with the exponent $\gamma = 3$. The same degree exponent has been obtained in the famous Barabási-Albert (BA) model [6] as well as some other deterministic models [28, 24, 29, 30, 51, 52, 53, 54].

2.3 Clustering Coefficient

The clustering coefficient [55] of a node u with degree k_u is given by $C_u = 2e_u/[k_u(k_u - 1)]$, where e_u is the number of existing links among the k_u neighbors. Using the construction rules, it is straightforward to calculate analytically the clustering coefficient $C(k)$ for a single node with degree k . For the initial two nodes born at step 0, their degree is $k = 2^t$, and the existing links among these neighbors is $\frac{k}{2}$, all of which are noniterated links. For those nodes created at step ϕ ($0 < \phi < t$), there are only $\frac{k-1}{2}$ links that actually exist among the neighbor nodes. Finally, for the smallest nodes created at step t , each has a degree of $k = 3$, the existing number of links between the neighbors of each is 2. Thus, there is a one-to-one correspondence between the clustering coefficient $C(k)$ of the node and its degree k :

$$C(k) = \begin{cases} 1/(k-1) & \text{for } k = 2^t \\ 1/k & \text{for } k = 2^m + 1 (2 \leq m \leq t) \\ 2/k & \text{for } k = 2^1 + 1 \end{cases} \quad (11)$$

which is inversely proportional to k in the limit of large k . The scaling of $C(k) \sim k^{-1}$ has been observed in many real-world scale-free networks [39].

Using Eq. (11), we can obtain the clustering C_t of whole the network at step t , which is defined as the average clustering coefficient of all individual nodes. Then we have

$$C_t = \frac{1}{N_t} \left[\frac{L_v(0)}{D_0 - 1} + \sum_{r=1}^{t-1} \frac{L_v(r)}{D_r} + \frac{2L_v(t)}{D_t} \right], \quad (12)$$

where D_r is the degree of a node at time t , which was created at step r , see Eq. (7). In the infinite network order limit ($N_t \rightarrow \infty$), Eq. (12) converges to a nonzero value $\bar{C} = 0.5435$. Therefore, the average clustering coefficient of the network is very high.

2.4 Fractal dimension

As a matter of fact, the fractal graph grows as an inverse renormalization procedure, see Fig. 2 in reverse order. To find the fractal dimension, we follow the mathematical framework presented in Ref. [18]. By construction, in the infinite t limit, the different quantities grow as:

$$\begin{cases} N_t \simeq 4 N_{t-1}, \\ k_u(t) \simeq 2 k_u(t-1), \\ \mathbb{D}_t = 2 \mathbb{D}_{(t-1)}, \end{cases} \quad (13)$$

where the third equation describes the change of the diameter \mathbb{D}_t of the graph F_t , where \mathbb{D}_t is defined as the longest shortest path between all pairs of nodes in F_t .

From the relations provided by Eq. (13), it is clear that the quantities N_t , $k_u(t)$ and \mathbb{D}_t increase by a factor of $f_N = 4$, $f_k = 2$ and $f_{\mathbb{D}} = 2$, respectively. Then between

any two times t_1, t_2 ($t_1 < t_2$), we can easily obtain the following relation:

$$\begin{cases} \mathbb{D}_{t_2} = 2^{t_2-t_1} \mathbb{D}_{t_1}, \\ N_{t_2} = 4^{t_2-t_1} N_{t_1}, \\ k_u(t_2) = 2^{t_2-t_1} k_u(t_1). \end{cases} \quad (14)$$

From Eq. (14), we can derive the scaling exponents in terms of the microscopic parameters: the fractal dimension is $d_B = \frac{\ln f_N}{\ln f_D} = 2$, and the degree exponent of boxes is $d_k = \frac{\ln f_k}{\ln f_D} = 1$. The exponent of the degree distribution satisfies $\gamma = 1 + \frac{d_B}{d_k} = 3$, giving the same γ as that obtained in the direct calculation of the degree distribution, see Eq. (10).

Note that in a class of deterministic models called pseudo-fractals, although the number of their nodes increases exponentially, the additive growth of the diameter with time implies that the networks are small world. These models do not capture the fractal topology found in diverse complex networks [32, 33, 34, 35, 36, 37, 40, 41, 42, 43].

2.5 Degree correlation

Degree correlation [56, 57, 58, 59, 60, 61, 62, 63] is a particularly interesting subject in the field of complex networks, because it can give rise to some interesting network structure effects. Degree correlation in a network can be measured by means of the quantity, called *average nearest-neighbor degree* (ANND) and denoted as $k_{nn}(k)$, which is a function of node degree, and is more convenient and practical in characterizing degree correlation. ANND is defined by [57]

$$k_{nn}(k) = \sum_{k'} k' P(k'|k), \quad (15)$$

where $P(k'|k)$ is the probability that a link from a node of degree k points to a node of degree k' .

For the fractal graph considered here, one can exactly calculate $k_{nn}(k)$. By construction, all neighbors of the initial two nodes have the same degree 3, while for each other nodes with degree greater than 3, only one of its neighbor has the same degree as itself, all the rest neighbors have a degree 3. Then we have

$$\begin{cases} k_{nn}(k) = 3 & \text{for } k = 2^t \\ k_{nn}(k) = 4 - \frac{3}{k} & \text{for } k = 2^m + 1 (m = 2, 3 \dots t). \end{cases} \quad (16)$$

For those nodes with degree 3, it is easily to obtain

$$\begin{aligned} k_{nn}(3) &= \frac{2 \cdot (2^t)^2 + \sum_{\tau=1}^{\tau=t-1} [L_v(\tau) k(\tau, t) [k(\tau, t) - 1]]}{3L_v(t)} + 1 \\ &= \frac{4}{3}t + \frac{5}{3} - \frac{4}{3} \cdot \frac{1}{2^t}, \end{aligned} \quad (17)$$

where $k(\tau, t)$ is the degree of a node at time t that was born at step τ . Thus $k_{nn}(3)$ grows linearly with time for large t . Eqs. (16) and (17) show the network is disassortative.

Degree correlation can also be described by a Pearson correlation coefficient r of degrees at either end of a link. It is defined as [59, 60, 42, 64]

$$r = \frac{\langle k \rangle \langle k^2 k_{nn}(k) \rangle - \langle k^2 \rangle^2}{\langle k \rangle \langle k^3 \rangle - \langle k^2 \rangle^2}. \quad (18)$$

We can easily see that for $t > 1$, r of F_t is always negative, indicating disassortativity.

2.6 Average path length

We represent all the shortest path lengths of F_t as a matrix in which the entry d_{ij} is the shortest path from node i to j . A measure of the typical separation between two nodes in F_t is given by the average path length (APL) \bar{d}_t , also known as characteristic path length [5], defined as the mean of geodesic lengths over all couples of nodes. APL is relevant in many fields regarding real-life networks and has received much attention [65, 66, 67, 68]. In the Appendix, we have obtained exact analytic expression for \bar{d}_t , which reads

$$\bar{d}_t = \frac{(16 \cdot 2^t + 21)16^t + (21t - 27)8^t + 75 \cdot 4^t + 119 \cdot 2^t - 15}{21(2 + 5 \cdot 4^t + 2 \cdot 16^t)}. \quad (19)$$

For large t , $\bar{d}_t \rightarrow \frac{8}{21} \cdot 2^t$. Note that in the infinite t limit, $N_t \sim 4^t$, so the APL scales as $\bar{d}_t \sim N_t^{1/2}$, which indicates that the network is not a small world.

Thus, we have shown that \bar{d}_t has the power-law scaling behavior of the number of nodes N_t , which is similar to that of two-dimensional regular lattice [69]. This phenomenon is not hard to understand. Let us look at the scheme of the network growth. Each next step in the growth of F_t doubles the APL between a fixed pair of nodes (except those small number of pairs directly connected by a noniterated link), while the total number of nodes increases four-fold (asymptotically, in the infinite limit of t), see Eq. (3). Thus the APL \bar{d}_t of F_t grows as a square power of the node number in the network.

3 SIR model on the network

As discussed in previous section, the network exhibits many interesting properties, i.e., it is simultaneously scale-free, highly clustered, ‘‘large-world’’, fractal and disassortative, which is not observed in uncorrelated networks with purely random wiring. Therefore, it is worthwhile to investigate the processes taking place upon the model to find the different impact on dynamic precesses compared with uncorrelated networks. In what follows we will study the SIR model of epidemics, which is one of the first issues to be explored in the literature on complex networks [13, 14, 15].

In the standard SIR model [16], each node of the network represents an individual and each link is the connection along which the individuals interact and the epidemic can be transmitted. This model describes diseases

resulting in the immunization or death of infected individuals, and assumes that each individual can be in one of three possible states, namely, susceptible, infected, and removed. The disease transmission on the network is described in an effective way: At each time step, each susceptible node is infected with probability λ , if it is connected to one or more infected nodes; at the same time, each infected individual becomes removed with probability 1, therefore it can not catch the infection again.

The SIR model is equivalent to a bond percolation problem with bond occupation probability λ [70, 71]. Moreover, the size of the outbreak is just the size of the giant component. In our case the percolation problem can be solved using the real-space renormalization group technique [72, 73, 74, 30], giving exact solution for the interesting quantity of epidemic threshold. Let us describe the procedure in application to the considered network. Assuming that the network growth stops at a time step $t \rightarrow \infty$, when the network is spoiled in the following way: for a link present in the undamaged network, with the probability λ we retain it in the damaged network. Then we invert the transformation in Fig. 2 and define $n = t - \tau$ for this inverted transformation, which is actually a decimation procedure [74]. Further, we introduce the probability λ_n that if two nodes are connected in the undamaged network at $\tau = t - n$, then at the n th step of the decimation for the damaged network, there exists a path between these vertices. Here, $\lambda_0 = \lambda$. We can easily obtain the following recursion relation for λ_n

$$\begin{aligned} \lambda_{n+1} &= \lambda_n^5 + 5\lambda_n^4(1 - \lambda_n) + 8\lambda_n^3(1 - \lambda_n)^2 + 2\lambda_n^2(1 - \lambda_n)^3 \\ &= 2\lambda_n^5 - 5\lambda_n^4 + 2\lambda_n^3 + 2\lambda_n^2. \end{aligned} \quad (20)$$

Equation (20) has an unstable fixed point at $\lambda_c = \frac{1}{2}$, and two stable fixed points at $\lambda = 0$ and $\lambda = 1$.

Thus, for the SIR model the epidemic prevalence undergoes a phase transition at a finite threshold λ_c of the transmission probability. If infection rate $\lambda > \lambda_c$, the disease spreads and infects a finite fraction of the population. On the other hand, when $\lambda < \lambda_c$, the total number of infected individuals is infinitesimally small in the limit of very large populations. The existence of an epidemic threshold in the present network is compared to the result for uncorrelated scale-free networks, where arbitrarily small infection rate λ shows finite prevalence [13, 14, 15].

Why uncorrelated scale-free networks are prone to epidemics spreading, while the present fractal disassortative scale-free network can suppress disease propagation? This may be explained as follows. In non-fractal uncorrelated scale-free topologies, the hubs are connected and form a central compact core, such that the infection of a few of the largest hubs has catastrophic consequences for the network. For the fractal network, it is disassortative and self-similar, which do not allow the presence of direct connections between hubs, i.e., hubs are more dispersed (see Fig. 2). Thus, the mixture of fractal and disassortative properties significantly provide protection against disease spreading. This could provide insight into explaining why some real-life networks have evolved into a fractal and disassortative architecture [17, 18].

4 Conclusions and discussion

To conclude, we have investigated a class of deterministic graphs from the viewpoint of complex networks. The deterministic self-similar construction allow us to derive analytic exact expressions for the relevant features. We have shown that the graphs simultaneously exhibit many interesting structural characteristics: power-law degree distribution, large clustering coefficient, ‘large-world’ phenomenon, fractal similar structure, negative degree correlations. The simultaneous existence of scale-free, high clustering, and ‘large-world’ behaviors is compared with previous network models.

Moreover, we have studied the SIR model in the graph under consideration. We have presented the presence of a finite epidemic threshold in the finite network size limit, showing that being prone to disease spreading is not an intrinsic property of scale-free networks. The ability of suppressing epidemic spreading may be owing to its inherent topologies. Thus, our research may be helpful for designing real networks resistant to epidemic outbreaks, and for the better understanding of the role that network structure plays in the spread of disease.

Although we have studied only a particular network corresponding to $q = 1$, in a similar way, one can easily investigate other networks (i.e., $q \geq 2$ cases) with various values of γ and d_B , and their general properties such as ‘large-world’ behavior, high clustering coefficient, and disassortative phenomenon are similar. Analogously, one can also analyze the SIR model on top of these networks. There is an existence of a different finite epidemic thresholds for all the cases, which depend on the parameter q . We speculate that the fractal property of the graphs determines the presence of the threshold of disease transmission for SIR model that can be mapped to a bond percolation as in the $d_B = \frac{\ln(4q)}{\ln 2}$ dimensional regular lattices [69]. In the end, we should mention that since most real-world networks are stochastic, it would be interesting to construct random network models displaying similar structural features as the deterministic model studied in the present work.

Acknowledgment

This research was supported by the National Basic Research Program of China under grant No. 2007CB310806, the National Natural Science Foundation of China under Grant Nos. 60496327, 60573183, 90612007, 60773123, and 60704044, the Postdoctoral Science Foundation of China under Grant No. 20060400162, the Program for New Century Excellent Talents in University of China (NCET-06-0376), and the Huawei Foundation of Science and Technology (YJCB2007031IN).

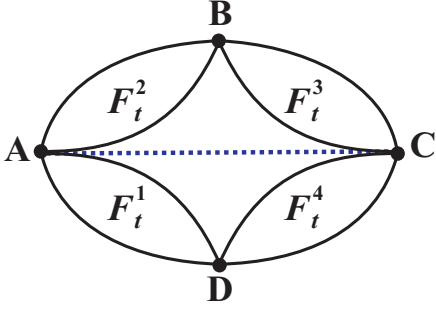


Fig. 3. (Color online) Second construction method of the network that highlights self-similarity: The graph after $t + 1$ construction steps, F_{t+1} , is composed of four copies of F_t denoted as F_t^α ($\alpha = 1, 2, 3, 4$), which are connected to one another as above. The blue dashed link is noniterated edge.

Appendix A: Derivation of the average path length

By definition, the APL for F_t is defined as follows

$$\bar{d}_t = \frac{D_t}{N_t(N_t - 1)/2}, \quad (21)$$

where

$$D_t = \sum_{i \in F_t, j \in F_t, i \neq j} d_{ij} \quad (22)$$

denotes the sum of the chemical distances between two nodes over all pairs, and d_{ij} is the chemical distance between nodes i and j . The network has a self-similar structure allowing one to calculate \bar{d}_t analytically. As shown in Fig. 3, the lattice F_{t+1} may be obtained by the juxtaposition of four copies of F_t , which are labeled as L_t^α , $\alpha = 1, 2, 3, 4$. Then we can write the sum D_{t+1} as

$$D_{t+1} = 4D_t + \Delta_t, \quad (23)$$

where Δ_t is the sum over all shortest paths whose endpoints are not in the same F_t branch. The solution of Eq. (23) is

$$D_t = 4^{t-1}D_1 + \sum_{x=1}^{t-1} 4^{t-x-1}\Delta_x. \quad (24)$$

The paths that contribute to Δ_t must all go through at least one of the four edge nodes (**A**, **B**, **C**, **D**, see Fig. 3) at which the different F_t branches are connected. The analytical expression for Δ_t , called the crossing paths, is found below.

Denote $\Delta_t^{\alpha,\beta}$ as the sum of all shortest paths with endpoints in F_t^α and F_t^β . If F_t^α and F_t^β meet at an edge node, $\Delta_t^{\alpha,\beta}$ rules out the paths where either endpoint is that shared edge node. If F_t^α and F_t^β do not meet, $\Delta_t^{\alpha,\beta}$ excludes the paths where either endpoint is any edge node. Then the total sum Δ_t is

$$\Delta_t = \Delta_t^{1,2} + \Delta_t^{1,3} + \Delta_t^{1,4} + \Delta_t^{2,3} + \Delta_t^{2,4} + \Delta_t^{3,4} - 2^{t+1} - 1, \quad (25)$$

The last two terms at the end compensate for the overcounting of certain paths: the shortest path between **B** and **D**, with length 2^{t+1} , is included in $\Delta_t^{1,2}$ and $\Delta_t^{3,4}$; the shortest path between **A** and **C**, with unit length 1, is included in both $\Delta_t^{1,4}$ and $\Delta_t^{2,3}$.

By symmetry, $\Delta_n^{1,2} = \Delta_n^{3,4}$, $\Delta_t^{1,3} = \Delta_t^{2,4}$ and $\Delta_t^{1,4} = \Delta_t^{2,3}$, so that

$$\Delta_t = 2\Delta_t^{1,2} + 2\Delta_t^{1,3} + 2\Delta_t^{1,4} - 2^{t+1} - 1, \quad (26)$$

where $\Delta_t^{1,2}$ is given by the sum

$$\begin{aligned} \Delta_t^{1,2} &= \sum_{\substack{i \in F_t^1, j \in F_t^2 \\ i, j \neq A}} d_{ij} \\ &= \sum_{\substack{i \in F_t^1, j \in F_t^2 \\ i, j \neq A}} (d_{iA} + d_{Aj}) \\ &= (N_t - 1) \sum_{i \in F_t^1} d_{iA} + (N_t - 1) \sum_{j \in F_t^2} d_{Aj} \\ &= 2(N_t - 1) \sum_{i \in F_t^1} d_{iA}, \end{aligned} \quad (27)$$

where $\sum_{i \in F_t^1} d_{iA} = \sum_{j \in F_t^2} d_{Aj}$ has been used. To find $\sum_{i \in F_t^1} d_{iA}$, we examine the structure of the graph at the t th level. In F_t^1 , there are $\nu_t(m)$ points with $d_{iA} = m$, where $1 \leq m \leq 2^t$, and $\nu_t(m)$ can be written recursively as

$$\nu_t(m) = \begin{cases} 2^t & \text{if } m \text{ is odd,} \\ \nu_{t-1}(\frac{m}{2}) & \text{if } m \text{ is even.} \end{cases} \quad (28)$$

We can write $\sum_{i \in F_t^1} d_{iA}$ in terms of $\nu_t(m)$ as

$$b_t \equiv \sum_{i \in F_t^1} d_{iA} = \sum_{m=1}^{2^t} m \cdot \nu_t(m). \quad (29)$$

Eqs. (28) and (29) relate b_t and b_{t-1} , which allow one to resolve b_t by induction as follow:

$$\begin{aligned} b_t &= \sum_{k=1}^{2^{t-1}} (2k-1) \cdot 2^t + \sum_{k=1}^{2^{t-1}} 2k \cdot \nu_{t-1}(k) \\ &= 2^{3t-2} + 2b_{t-1} = \frac{1}{3} 2^t (2 + 4^t), \end{aligned} \quad (30)$$

where $b_1 = \nu_1(1) + 2\nu_1(2) = 4$ has been used. Substituting Eq. (30) and $N_t = \frac{2}{3}(2 + 4^t)$ into Eq. (27), we obtain

$$\Delta_t^{1,2} = \frac{1}{9} 2^{t+1} (2^{1+2t} + 1) (4^t + 2). \quad (31)$$

Continue analogously,

$$\begin{aligned}
\Delta_t^{1,4} &= \sum_{\substack{i \in F_t^1, i \neq A, D \\ j \in F_t^4, j \neq C, D}} d_{ij} \\
&= \sum_{\substack{i \in F_t^1, i \neq A \\ j \in F_t^4, j \neq C \\ d_{iA} + d_{jC} < 2^t}} (d_{iA} + d_{jC}) + \sum_{\substack{i \in F_t^1, i \neq A \\ j \in F_t^4, j \neq C \\ d_{iA} + d_{jC} < 2^t}} d_{AC} \\
&\quad + \sum_{\substack{i \in F_t^1, i \neq A \\ j \in F_t^4, j \neq C \\ d_{iC} + d_{jC} = 2^t}} 2^t + \sum_{\substack{i \in F_t^1, i \neq A \\ j \in F_t^4, j \neq C \\ d_{iC} + d_{jC} > 2^t}} (d_{iD} + d_{jD}) \\
&\quad + \sum_{i \in F_t^1} d_{iC} + \sum_{j \in F_t^4} d_{jA} - 2 \cdot 2^t - 1, \quad (32)
\end{aligned}$$

The first term equals the fourth one and is denoted by g_t . The second and third terms are denoted by y_t and h_t , respectively. The fifth and sixth terms are equal to each other, both of which equal to $b_t + N_t - 1$. The last two terms at the end compensate for the redundancy or overcounting of certain paths: the shortest paths of d_{CD} in $\sum_{i \in F_t^1} d_{iC}$ and d_{AD} in $\sum_{j \in F_t^4} d_{jA}$ are redundant, both of which are 2^t ; the shortest path between d_{AC} with unit length 1 is included in both $\sum_{i \in F_t^1} d_{iC}$ and $\sum_{j \in F_t^4} d_{jA}$. Therefore $\Delta_t^{1,4} = 2g_t + h_t + y_t + 2b_t - 2^{t+1} + 2N_t - 3$. One can compute the quantity g_t as

$$\begin{aligned}
g_t &= \sum_{m=1}^{2^{t-2}} \sum_{m'=1}^{2^{t-1}-m} \nu_t(m) \nu_t(m') (m + m') \\
&= \sum_{k=1}^{2^{t-1}-2} \sum_{k'=1}^{2^{t-1}-1-k} \nu_{t-1}(k) \nu_{t-1}(k') (2k + 2k') \\
&\quad + \sum_{k=1}^{2^{t-1}-1} \sum_{k'=1}^{2^{t-1}-k} \nu_{t-1}(k) 2^t (2k + 2k' - 1) \\
&\quad + \sum_{k=1}^{2^{t-1}-1} \sum_{k'=1}^{2^{t-1}-k} 2^t \nu_{t-1}(k') (2k - 1 + 2k') \\
&\quad + \sum_{k=1}^{2^{t-1}-1} \sum_{k'=1}^{2^{t-1}-k} 2^{2t} (2k - 1 + 2k' - 1), \quad (33)
\end{aligned}$$

where the fourth term can be summed directly, yielding

$$\frac{1}{3} 2^{-2+3t} (-2 + 2^t) (-1 + 2^t). \quad (34)$$

In Eq. (33), the second and third terms are equal to each other and can be simplified by first summing over k' , yielding

$$2^t \sum_{k=1}^{2^{t-1}-1} \nu_{t-1}(k) (4^t - k^2). \quad (35)$$

For use in Eq. (35), $\sum_{k=1}^{2^{t-1}-1} \nu_{t-1}(k) = N_{t-1} - 2$. On the other hand, it is easy to derive the following recursive

relation

$$\sum_{k=1}^{2^{t-1}} k^2 \nu_{t-1}(k) = \sum_{z=1}^{2^{t-2}} (2z-1)^2 2^{t-1} + \sum_{z=1}^{2^{t-2}} (2z)^2 \nu_{t-2}(k), \quad (36)$$

using which we have

$$\begin{aligned}
\sum_{k=1}^{2^{t-1}-1} k^2 \nu_{t-1}(k) &= \sum_{k=1}^{2^{t-1}} k^2 \nu_{t-1}(k) - 2^{2t-2} \\
&= \frac{1}{9} 2^{2t-3} (4^t - 3t + 17) - 2^{2t-2}. \quad (37)
\end{aligned}$$

With these results, Eq. (35) becomes

$$\frac{1}{9} 8^{-1+t} (-11 + 2^{1+2t} + 3t). \quad (38)$$

With Eqs. (34) and (38), Eq. (33) becomes

$$g_t = 2g_{t-1} + \frac{2^t}{36} (5 \cdot 16^t - 5 \cdot 4^t - 9 \cdot 8^t + 3t \cdot 4^t). \quad (39)$$

Considering the initial condition $g_1 = 0$, we can solve Eq. (39) inductively leading to

$$g_t = \frac{1}{945} 2^t (158 + 112 \cdot 16^t - 270 \cdot 8^t + 210t \cdot 4^{t-1}). \quad (40)$$

We now evaluate h_t using a recursive method:

$$\begin{aligned}
h_t &= 2^t \sum_{m=1}^{2^{t-1}} \nu_t(m) \nu_t(2^t - m) \\
&= 2^t \sum_{m=1}^{2^{t-1}} \nu_t^2(m) \\
&= 2^t \left[\sum_{k=1}^{2^{t-1}} 4^t + \sum_{k=1}^{2^{t-1}-1} \nu_{t-1}^2(k) \right] \\
&= 2^{4t-1} + 2h_{t-1}, \quad (41)
\end{aligned}$$

where we have used the symmetry $\nu_t(m) = \nu_t(2^t - m)$. Since $h_1 = 8$, Eq. (41) is solved inductively:

$$h_t = 2^{t+2} (8^t - 1) / 7. \quad (42)$$

To find an expression for $\Delta_t^{1,4}$, now the only thing left is to evaluate y_t , which can be calculated using the same way

as g_t . Replacing $m + m'$ in Eq. (33) with 1, one can get

$$\begin{aligned}
y_t &= \sum_{m=1}^{2^t-2} \sum_{m'=1}^{2^t-1-m} \nu_t(m)\nu_t(m') \\
&= \sum_{k=1}^{2^{t-1}-2} \sum_{k'=1}^{2^{t-1}-1-k} \nu_{t-1}(k)\nu_{t-1}(k') \\
&\quad + \sum_{k=1}^{2^{t-1}-1} \sum_{k'=1}^{2^{t-1}-k} \nu_{t-1}(k)2^t \\
&\quad + \sum_{k=1}^{2^{t-1}-1} \sum_{k'=1}^{2^{t-1}-k} 2^t \nu_{t-1}(k') \\
&\quad + \sum_{k=1}^{2^{t-1}-1} \sum_{k'=1}^{2^{t-1}-k} 2^{2t}(2k-1+2k'-1). \quad (43)
\end{aligned}$$

Analogously to the computation of g_t , we can easily obtain

$$y_t = \frac{2}{63}(-1+2^t)(7 \cdot 8^t - 2 \cdot 4^t - 16 \cdot 2^t - 16) \quad (44)$$

Combining previous equations and results, we get the final expression for $\Delta_t^{1,4}$,

$$\begin{aligned}
\Delta_t^{1,4} &= \frac{1}{189} \left(33 - 98 \cdot 2^t + 168 \cdot 2^{2t} - 12 \cdot 2^{3t} - 66 \cdot 2^{4t} \right. \\
&\quad \left. + 56 \cdot 2^{5t} + 108 \cdot 4^{2t} + 42t \cdot 2^{3t} \right). \quad (45)
\end{aligned}$$

We now begin to compute $\Delta_t^{1,3}$, which can be obtained from $\Delta_t^{1,2}$ by regarding A and C as one single point, plus d_{AC} to the path length of all related pairs of nodes, so that

$$\begin{aligned}
\Delta_t^{1,3} &= \Delta_t^{1,2} + (N_t - 2)^2 - 2[b_t + 2^t(N_t - 1)] + 2^{t+1} \\
&= \frac{4}{9} \left(1 + 2^t - 2^{1+2t} - 2^{1+3t} + 2^{4t} + 2^{5t} \right). \quad (46)
\end{aligned}$$

Substituting Eqs. (31), (45) and (46) into Eq. (26), we obtain the final expression for the crossing paths Δ_t :

$$\begin{aligned}
\Delta_t &= \frac{1}{189} \left[45 - 119 \cdot 2^{t+1} + 15 \cdot 2^{3t+2} + 7 \cdot 2^{5t+6} \right. \\
&\quad \left. + 63 \cdot 4^{2t+1} + 21t \cdot 2^{3t+2} \right]. \quad (47)
\end{aligned}$$

Substituting Eqs. (47) for Δ_x into Eq. (24), and using $D_0 = 1$, we have

$$\begin{aligned}
D_t &= \frac{1}{189} \left[2^{4+5t} + 21 \cdot 2^{4t} + 21t \cdot 2^{3t} - 27 \cdot 2^{3t} \right. \\
&\quad \left. + 75 \cdot 2^{2t} + 119 \cdot 2^t - 15 \right]. \quad (48)
\end{aligned}$$

Inserting Eq. (48) into Eq. (21), one can obtain the analytical expression for \bar{d}_t in Eq. (19).

References

1. R. Albert and A.-L. Barabási, Rev. Mod. Phys. **74**, 47 (2002).
2. S.N. Dorogovtsev and J.F.F. Mendes, Adv. Phys. **51**, 1079 (2002).
3. M.E.J. Newman, SIAM Rev. **45**, 167 (2003).
4. S. Boccaletti, V. Latora, Y. Moreno, M. Chavez and D.-U. Hwang, Phys. Rep. **424**, 175 (2006).
5. L. da F. Costa, F.A. Rodrigues, G. Travieso, and P.R.V. Boas, Adv. Phys. **56**, 167 (2007).
6. A.-L. Barabási and R. Albert, Science **286**, 509 (1999).
7. R. Albert, H. Jeong, A.-L. Barabási, Nature (London) **406**, 378 (2000).
8. D. S. Callaway, M. E. J. Newman, S. H. Strogatz, and D. J. Watts, Phys. Rev. Lett. **85**, 5468 (2000).
9. R. Cohen, K. Erez, D. ben-Avraham, and S. Havlin, Phys. Rev. Lett. **86**, 3682 (2001).
10. M. Barahona and L. M. Pecora, Phys. Rev. Lett. **89**, 054101 (2002).
11. X. F. Wang, G. Chen, IEEE Trans. Circuits Syst. I **49**, 54 (2002).
12. G. Szabó and G. Fátth, Phys. Rep. **446**, 97 (2007).
13. R. Pastor-Satorras and A. Vespignani, Phys. Rev. Lett. **86**, 3200 (2001).
14. R. Pastor-Satorras and A. Vespignani, Phys. Rev. E **63**, 066117 (2001).
15. Y. Moreno, R. Pastor-Satorras, and A. Vespignani, Eur. Phys. J. B **26**, 521 (2002).
16. H. W. Hethcote, SIAM Rev. **42**, 599 (2000).
17. C. Song, S. Havlin, H. A. Makse, Nature **433**, 392 (2005).
18. C. Song, S. Havlin, H. A. Makse, Nature Phys. **2**, 275 (2006).
19. S.-H. Yook, F. Radicchi, and H. M.-Ortmanns, Phys. Rev. E **72**, 045105(R) (2006).
20. K.-I. Goh, G. Salvi, B. Kahng and D Kim, Phys. Rev. Lett. **96**, 018701 (2006).
21. C. Song, L. K. Gallos, S. Havlin, H. A. Makse, J. Stat. Mech.:Theory Exp. **P03006**, (2007).
22. J. S. Kim, K.-I. Goh, B. Kahng, and D Kim, Chaos **17**, 026116 (2007).
23. M. Kitsak, S. Havlin, G. Paul, M. Riccaboni, F. Pammolli, and H. E. Stanley, Phys. Rev. E **75**, 056115 (2007).
24. Z. Z. Zhang, S. G. Zhou, and T. Zou, Eur. Phys. J. B **56**, 259 (2007).
25. L. Barrière, F. Comellas, and C. Dalfó, J. Phys. A, **39**, 11739 (2006).
26. L. K. Gallos, C. Song, S. Havlin, H. A. Makse, Proc. Natl Acad. Sci. USA **10**, 7746 (2007).
27. S. Condamin, O. Bénichou, V. Tejedor, R. Voituriez, and J. Klafter, Nature **450**, 77 (2007).
28. M. Hinczewski, Phys. Rev. E **75**, 061104 (2007).
29. H. D. Rozenfeld, S. Havlin, and D. ben-Avraham, New J. Phys. **9**, 175 (2007).
30. H. D. Rozenfeld and D. ben-Avraham, Phys. Rev. E **75**, 061102 (2007).
31. A.-L. Barabási, E. Ravasz, and T. Vicsek, Physica A **299**, 559 (2001).
32. S. N. Dorogovtsev, A. V. Goltsev, and J. F. F. Mendes, Phys. Rev. E **65**, 066122 (2002).
33. F. Comellas, G. Fertin and A. Raspaud, Phys. Rev. E **69**, 037104 (2004).

34. Z. Z. Zhang, L. L. Rong, and S. G. Zhou, *Physica A* **377** (2007) 329.
35. Z. Z. Zhang, S. G. Zhou, and L. C. Chen, *Eur. Phys. J. B* **58**, 337 (2007).
36. S. Jung, S. Kim, and B. Kahng, *Phys. Rev. E* **65**, 056101 (2002).
37. Z. Z. Zhang, S. G. Zhou, L. C. Chen, J. H. Guan, L. J. Fang, and Y. C. Zhang, *Eur. Phys. J. B* **59**, 99 (2007).
38. E. Ravasz, A.L. Somera, D.A. Mongru, Z.N. Oltvai, and A.-L. Barabási, *Science* **297**, 1551 (2002).
39. E. Ravasz and A.-L. Barabási, *Phys. Rev. E* **67**, 026112 (2003).
40. Z.Z. Zhang, S.G. Zhou, L.J. Fang, J.H. Guan, and Y.C. Zhang, *Europhys. Lett.* **79**, 38007 (2007).
41. J. S. Andrade Jr., H. J. Herrmann, R. F. S. Andrade and L. R. da Silva, *Phys. Rev. Lett.* **94**, 018702 (2005).
42. J. P. K. Doye and C. P. Massen, *Phys. Rev. E* **71**, 016128 (2005).
43. Z. Z. Zhang, F. Comellas, G. Fertin and L. L. Rong, *J. Phys. A* **39**, 1811 (2006).
44. Z. Z. Zhang, L. L. Rong, and S. G. Zhou, *Phys. Rev. E*, **74**, 046105 (2006).
45. F. Comellas, J. Ozón, and J. G. Peters, *Inf. Process. Lett.*, **76**, 83 (2000)
46. F. Comellas and M. Sampels, *Physica A* **309**, 231 (2002).
47. Z. Z. Zhang, L. L. Rong and C. H. Guo, *Physica A* **363**, 567 (2006).
48. T. Zhou, B. H. Wang, P. M. Hui and K. P. Chan, *Physica A* **367**, 613 (2006).
49. M. Chen, B.Yu, P. Xu, and J. Chen, *Physica A* **385**, 707 (2007).
50. Z. Z. Zhang, S. G. Zhou, Z. Y. Wang, and Z. Shen, *J. Phys. A: Math. Theor.* **40**, 11863 (2007).
51. A. N. Berker and S. Ostlund, *J. Phys. C* **12**, 4961 (1979).
52. M. Kaufman and R. B. Griffiths, *Phys. Rev. B* **24**, 496 (1981).
53. M. Hinczewski and A. N. Berker, *Phys. Rev. E* **73**, 066126 (2006).
54. Z. R. Yang, *Phys. Rev. B* **38**, 728 (1988).
55. D.J. Watts and H. Strogatz, *Nature (London)* **393**, 440 (1998).
56. S. Maslov and K. Sneppen, *Science* **296**, 910 (2002).
57. R. Pastor-Satorras, A. Vázquez and A. Vespignani, *Phys. Rev. Lett.* **87**, 258701 (2001).
58. A. Vázquez, R. Pastor-Satorras and A. Vespignani, *Phys. Rev. E* **65**, 066130 (2002).
59. M. E. J. Newman, *Phys. Rev. Lett.* **89**, 208701 (2002).
60. M. E. J. Newman, *Phys. Rev. E* **67**, 026126 (2003).
61. M. Boguñá and R. Pastor-Satorras, *Phys. Rev. E* **68**, 036112 (2003).
62. A. Barrat and R. Pastor-Satorras, *Phys. Rev. E* **71**, 036127 (2005).
63. Z. Z. Zhang and S. G. Zhou, *Physica A*, **380**, 621 (2007).
64. J. J. Ramasco, S. N. Dorogovtsev, and R. Pastor-Satorras, *Phys. Rev. E* **70**, 036106 (2004).
65. A. Fronczak, P. Fronczak, and J. A. Hołyst, *Phys. Rev. E* **70**, 056110 (2004).
66. J. A. Hołyst, J. Sienkiewicz, A. Fronczak, P. Fronczak, and K. Suchecki, *Phys. Rev. E* **72**, 026108 (2005).
67. S. N. Dorogovtsev, J. F. F. Mendes, and J. G. Oliveira, *Phys. Rev. E* **73**, 056122 (2006).
68. Z.Z. Zhang, L.C. Chen, S.G. Zhou, L.J. Fang, J.H. Guan, and T. Zou, *Phys. Rev. E* **77**, 017102 (2008).
69. M. E. J. Newman, *J. Stat. Phys.* **101** 819 (2000).
70. P. Grassberger, *Math. Biosci.* **63**, 157 (1982).
71. M. E. J. Newman, *Phys. Rev. E* **66**, 016128 (2002).
72. A.A. Migdal, *Zh. Eksp. Teor. Fiz.* **69**, 1457 (1975) [*Sov. Phys. JETP* **42**, 743 (1976)].
73. L.P. Kadanoff, *Ann. Phys. (N.Y.)* **100**, 359 (1976).
74. S. N. Dorogovtsev, *Phys. Rev. E* **67**, 045102(R) (2003).

